Resistive wall wakefields of short bunches at cryogenic temperatures

LCLS-II TN-15-01

1/15/15

G. Stupakov, K. L. F. Bane, and P. Emma
SLAC National Accelerator Laboratory, Menlo Park, CA 94025, USA
B. Podobedov
Brookhaven National Laboratory, Upton, New York 11973, USA

LCLS-II-TN-15-01
SLAC-PUB-16197
January 2015

Resistive wall wakefields of short bunches at cryogenic temperatures

G. Stupakov, K. L. F. Bane, and P. Emma
SLAC National Accelerator Laboratory, Menlo Park, CA 94025, USA

B. Podobedov
Brookhaven National Laboratory, Upton, New York 11973, USA

Abstract

We present calculations of the longitudinal wakefields at cryogenic temperatures for extremely short bunches, characteristic for modern x-ray free electron lasers. The calculations are based on the equations for the surface impedance in the regime of the anomalous skin effect in metals. This work extends and complements an earlier analysis of Ref. [3] into the region of very high frequencies associated with bunch lengths in the micron range. We study in detail the case of a rectangular bunch distribution for parameters of interest of LCLS-II with a superconducting undulator.

I. INTRODUCTION

Resistive wall wakefields generated due to finite conductivity of an accelerator vacuum chamber often play an important role in beam dynamics [1, 2]. They become increasingly important for smaller apertures and shorter bunches. The techniques to evaluate these wakefields for the regime of normal skin effect (NSE) for various cross sections of the vacuum chamber are well developed. While the NSE regime commonly applies to accelerator components operating at room temperature, it generally does not hold when beam-exposed metal surfaces are at cryogenic temperatures. In the latter case, metals enter the anomalous skin effect regime (ASE) where the conductivity is substantially different from NSE. A detailed study [3] of wakefields in the ASE regime was conducted earlier by one of the co-authors of this paper (BP). In order to calculate the wakefields analytically, that work was restricted to the so-called "extreme" range of the ASE regime, where the surface impedance expressions can be significantly simplified. As a tradeoff, the results of [3] are not directly applicable to bunches shorter than approximately 0.1 ps rms, which is more than adequate for storage ring applications, such as those described in [3].

Another area where the ASE wakefields can play an important role is a small gap vacuum chamber of a superconducting undulator in a free electron laser [4]. The energy loss of the beam due to the resistive wall wakefield in the undulator interferes with the lasing process, and its knowledge and control is important for optimization of the FEL performance. The results of [3] cannot be directly used for very short bunches in x-ray FELs, where the typical bunch length could be as low as a few femtoseconds, and, in addition, the bunch shape is non-Gaussian, extending the bunch shape spectrum further in frequency. It is the goal of this paper to present numerical calculations of wakefields for such extremely short bunches in the ASE regime. We limit our consideration to the longitudinal wakefields; the transverse

wakes in the undulator are believed to be of lesser importance due to the shortness of the bunches.

The vacuum chamber within the superconducting undulator of LCLS-II will likely have a racetrack cross-section with a large ratio of horizontal to vertical dimensions. From an impedance point of view, with the beam on axis, the effect of the wakefield is essentially the same as for the case of flat geometry, i.e. for a chamber consisting of two parallel plates with the same vertical separation, which we denote by $2a$ (a is the half aperture). This is the model that we accept in this paper. For comparison, we also calculate the wakefields for a round geometry with the radius equal to a.

Selected beam and machine properties in the undulator region of LCLS-II that are used in our calculations are given in Table I [5]. We consider two options for the bunch charge—100 and 300 pC—each with the beam current of 1 kA.

TABLE I. Selected beam and machine properties in the undulator region of LCLS-II with superconducting undulator. The longitudinal bunch distribution is approximately uniform.

Parameter name	Value	Unit
Beam current, I	1	kA
Bunch charge, Q	100(300)	pC
RMS bunch length, σ_z	8.7(26)	μm
Beam energy, E	4	GeV
Vacuum chamber half aperture, a	2.5	mm
Undulator length, L	100	m

The paper is organized as follows. In Section II, we briefly review the anomalous skin effect and present the equation for the surface conductivity of the metal in this regime. In Section III, we calculate the impedance and wake of a point charge in ASE regime in a round vacuum chamber. In Section IV, we calculate the impedance

and wake in flat geometry, which is more relevant for the typical racetrack shape of an undulator vacuum chamber. Assuming parameters of the LCLS-II with a superconducting undulator, we also compute the relative energy change of electrons in the bunch. Section V summarizes the results of the paper.

II. ANOMALOUS SKIN EFFECT AND SURFACE IMPEDANCE

The classical skin depth $\delta^{\rm NSE}$ as a function of frequency ω is defined by the following formula,

$$\delta^{\rm NSE} = \sqrt{\frac{2c}{Z_0\sigma_c\omega}}, \tag{1}$$

where σ_c is the metal conductivity, Z_0 is the free space impedance, $Z_0 = 120\pi$ Ohm, and c is the speed of light. When the skin depth $\delta^{\rm NSE}$ becomes less than or comparable to the mean free-path of electrons l the classical model of the skin effect no longer holds [6, 7]. Different expressions for the skin effect are known for the cases of *specular* and *diffuse* reflection of electrons at the surface. Fitting these formulas to infrared measurements for Cu, Ag, Au, Lenham and Treherne concluded that the diffuse model is normally applicable, even for well-prepared samples [8]. This is the model we use in this paper.

The conductivity σ_c in the free-electron (Drude) model of metals is given by

$$\sigma_c = \frac{ne^2 l}{mv_f} = \frac{\omega_p^2 l}{Z_0 c v_f}, \tag{2}$$

where n is the concentration of conducting electrons, m is the effective mass, ω_p is the corresponding plasma frequency, l is the mean-free path of conducting electrons and v_f is the Fermi velocity. For reference, we list in Table II the free-electron model parameters for Al and Cu, which are two commonly used metals in accelerator applications. Conductivity of pure metals increases several orders of magnitude when they are cooled from room temperature to cryogenic temperatures,

where the conductivity is impurity dominated. A commonly used parameter, the residual resistivity ratio (RRR), is defined (at 4 K) as RRR $\equiv \sigma_c(4\,\mathrm{K})/\sigma_c(293\,\mathrm{K})$. Relevant for this paper is that bulk pieces of Cu and Al with RRR values of a hundred or more are commercially available for use in cryogenic components of accelerator vacuum chambers. In our calculations, we assume RRR = 100 with the room temperature conductivities $\sigma_c(293\,\mathrm{K}) = 5.7 \cdot 10^7$ (Ohm m)$^{-1}$ for copper and $\sigma_c(293\,\mathrm{K}) = 3.7 \cdot 10^7$ (Ohm m)$^{-1}$ for aluminum.

TABLE II. Free-electron Fermi gas model parameters for Al and Cu [9].

	n 10^{28} m^{-3}	v_f 10^6 m/s	ω_p 10^{16} rad/s
Al	18	2.0	2.4
Cu	8.5	1.6	1.7

Solving Maxwell's equations inside a metal chamber requires one to specify a relation between the tangential components of the electric $\boldsymbol{E}_t$ and magnetic $\boldsymbol{H}_t$ fields on the metal surface. At high frequencies, this relation is known as the Leontovich boundary condition [10]. In frequency representation it is given by the following equation:

$$\boldsymbol{E}_t = \zeta(\omega)[\boldsymbol{H}_t \times \boldsymbol{n}], \tag{3}$$

where $\boldsymbol{n}$ is a unit vector directed into the metal perpendicular to the surface and $\zeta(\omega)$ denotes the dimensionless surface impedance.

The ASE theory developed in [6, 7] gives the following expression for the complex conjugate of the surface impedance[1]:

$$\zeta^*(\omega) = -\frac{i\omega l}{cF(\omega)}, \tag{4}$$

[1] The complex conjugate appears here because of a different choice of the sign in the Fourier transforms in Refs. [6, 7].

where the function F is defined by

$$F(\omega) = -\frac{1}{\pi} u \int_0^\infty \ln\left[1 + \frac{\eta + \xi\varkappa(t)}{t^2}\right] dt, \tag{5}$$

with $u = 1 + i\omega l/v_f$, $\eta = -\omega^2 l^2/c^2 u^2$, $\varkappa(t) = 2t^{-3}[(1+t^2)\arctan(t) - t]$, $\xi = i\alpha u^{-3}$ and $\alpha = \frac{3}{2}(l/\delta^{\rm NSE})^2$. As discussed in [6], the parameter η is typically small in comparison with other terms in Eq. (5) and is neglected. In our calculations the value of the mean free path l in these equations was expressed through the conductivity σ_c = RRR $\cdot\, \sigma_c(293\ \mathrm{K})$ using Eq. (2) and parameters in Table II.

The case of extreme anomalous skin effect (EASE) studied in [3] is characterized by $|\xi| \gg 1$. In this limit Eq. (5) can be considerably simplified, $F(\omega) \approx -2(\pi\xi)^{1/3}/\sqrt{3}$. With this expression for F, one finds the surface impedance which coincides with Eq. (8) of Ref. [3]. As is pointed out in [3], the condition when one can use the EASE expression for the impedance is limited by the requirement $\omega \ll \omega_p v_f/c$ which constraints the applicability of EASE to bunches with rms length $\sigma \gg \sigma_0 \equiv c^2/\omega_p v_f$. To estimate this limit for our case, we take RRR = 100, and using parameters from Table II, find $\sigma_0 \approx 1.9$ μm for aluminum and $\sigma_0 \approx 3.3$ μm for copper as a lower limit of validity. Comparing these numbers with the shortest bunch length of 8.7 μm from Table I we see that the value of σ_z of interest is not quite in the regime of EASE. And indeed, we found a noticeable deviation of the wakefield for such short bunch from the result of EASE.

We mention in passing that the NSE regime is obtained from Eq. (5) in the limit $|\xi| \ll 1$. In this limit one can replace $\varkappa(t)$ in (5) by its value $\varkappa(0) = \frac{4}{3}$, which gives $F(\omega) \approx -2u\sqrt{\xi/3} = -2u^{-1/2}\sqrt{i\alpha/3}$. Substituting this expression into (4) gives $\zeta = (1-i)\omega\delta^{\rm NSE}u^{*1/2}/2c$ which is a standard expression for the surface impedance in the NSE regime with the correction that takes into account the frequency dependence of the conductivity (a so called *ac conductivity* [11]).

We should point out that Eqs. (4) and (5) were also used in [12] to calculate the wake effect for short bunches at room temperature, when the result was found to

agree well with the normal, NSE regime.

III. ROUND VACUUM CHAMBER

Consider first a round chamber of inner radius a. The beam impedance in this case is [1]

$$Z(k) = \frac{Z_0}{2\pi a}\left(\frac{1}{\zeta(k)} - \frac{ika}{2}\right)^{-1}, \tag{6}$$

where $k = \omega/c$, and we consider here ζ as a function of k, rather than the frequency ω, as defined by (4). Once the impedance is known, the wake is obtained by the inverse Fourier transform:

$$w(s) = \frac{c}{2\pi}\int_{-\infty}^{\infty} Z(k)e^{-iks}dk, \tag{7}$$

with s the distance the test particle is behind the driving particle. The wake defined by this equation has a property $w(s) = 0$ for $s < 0$, and a positive value of w indicates energy loss.

In Fig. 1 we show the real and imaginary parts of the impedance as a function of frequency for copper and aluminum for a pipe of radius $a = 2.5$ mm. Note that the impedance has a resonant-like character with the peak of the resonance located close to 10 THz. In Fig. 2 we show the corresponding wakes for a point charge. For comparison, on the same plot, we also show the wake for the case when the aluminum pipe is at room temperature (no ASE), repeating the calculation of Ref. [14]. Comparing the latter with the low-temperature wake, it might seem counterintuitive that the room-temperature wake is not too much different from the low-temperature limit, where the resistivity is hundred times smaller. We remind the reader however, that for extremely short distances of interest in this paper, the wake is not directly related to the wall conductivity. In particular, as one can see from Fig. 2, all the wakes are equal at the origin $s = 0$, where universally $w(0) = Z_0 c/\pi a^2$ (see, e.g., discussion in [13]).

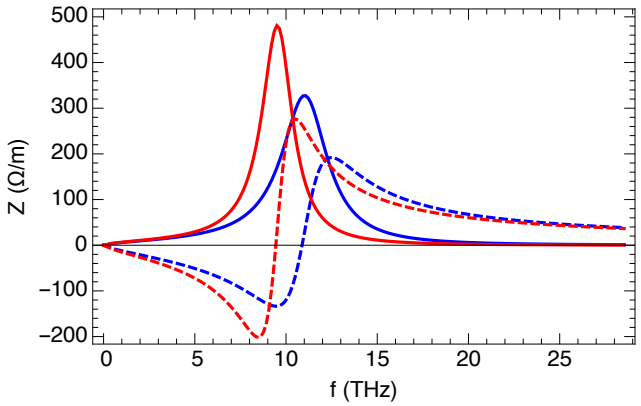

FIG. 1. For round geometry: real (solid lines) and imaginary (dashed lines) parts of the impedance (6) for copper (red) and aluminum (blue).

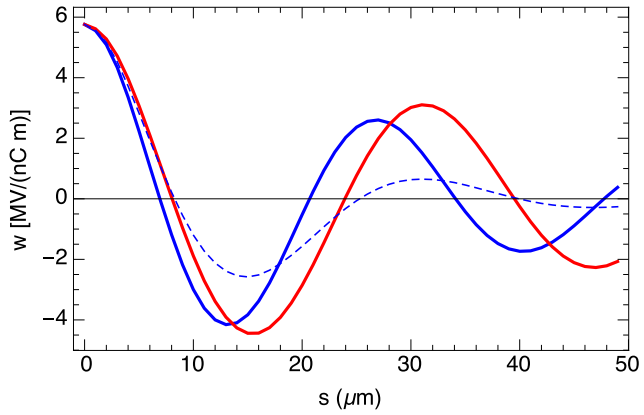

FIG. 2. The wake of the point charge for copper (red) and aluminum (blue) pipes. The dashed black line shows the wake for the case when the aluminum pipe is at room temperature (no ASE).

IV. FLAT VACUUM CHAMBER

The impedance of a resistive wall in flat geometry is given in Ref. [14],

$$Z(k) = \frac{Z_0}{2\pi a}\int_0^\infty \frac{dq}{\cosh(q)}\left[\frac{\cosh(q)}{\zeta(k)} - \frac{ika}{q}\sinh(q)\right]^{-1}. \tag{8}$$

Using Eqs. (4) and (5) for the surface impedance we numerically calculated the integral (8) as a function of k. In Fig. 3 we present the real and imaginary parts of Z as a function of frequency for copper and aluminum. In Fig. 4 we show the

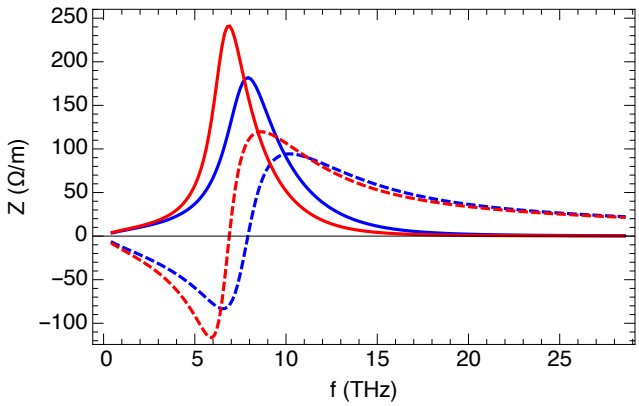

FIG. 3. For flat geometry: real (solid lines) and imaginary (dashed lines) parts of the impedance (8) for copper (red) and aluminum (blue).

corresponding wake for a point charge. For comparison, we also show the wake for the case when the aluminum pipe is at room temperature (no ASE).

As mentioned before, the bunch distribution in the undulator region of LCLS-II is approximately uniform. For a uniform bunch distribution with peak current I the relative wake induced energy variation $\eta = \Delta E/E$ at the end of the undulator is given by

$$\eta(z) = -\frac{eIL}{cE}\int_0^z w(s)ds, \tag{9}$$

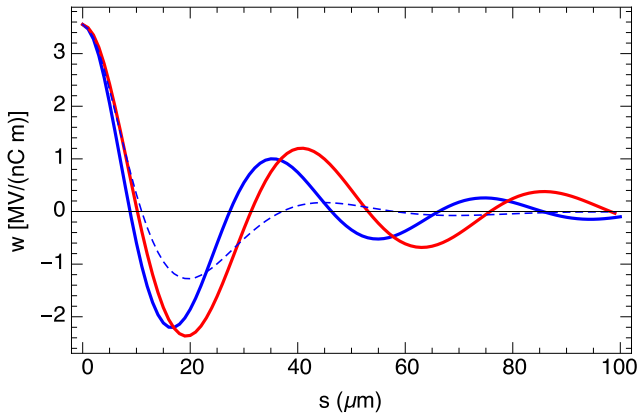

FIG. 4. For flat geometry: the wake of the point charge for copper (red) and aluminum (blue) pipes. The dashed black line shows the wake for the case when the aluminum pipe is at room temperature (no ASE).

with L the length of the undulator pipe and E the beam energy. In Fig. 5 we plot the relative energy change of electrons in the beam as a function of position in the bunch z. The energy $E = 4$ GeV, and the length of pipe $L = 100$ m. The beam has a uniform distribution with its head located at $z = 0$. Because we assume the same peak current $I = 1$ kA for the two cases $Q = 100$ pC and $Q = 300$ pC, the function $\eta(z)$ is the same for both of them, extending from 0 to 30 μm in the first case and from 0 to 90 μm in the second one. For comparison, we also show the warm wake result for aluminum as well as the relative energy change obtained in the EASE model of Ref. [3]. The discrepancy between the solid and dashed curves clearly shows that the EASE model is not applicable for the extremely short bunches of interest for this work.

Using the results shown in Fig. (5) we calculated the average energy loss $\eta_{\rm av}$ and the rms energy spread σ_η at the end of the undulator due to the wake. For the bunch charge of 100 pC they are: for Cu $\eta_{\rm av} = -0.076\%$, $\sigma_\eta = 0.085\%$; for Al $\eta_{\rm av} = -0.052\%$, $\sigma_\eta = 0.077\%$. The same quantities for a bunch charge of 300 pC

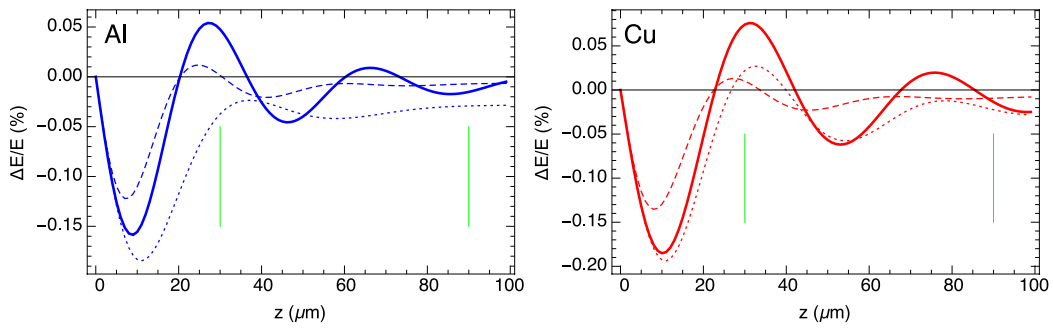

FIG. 5. For flat geometry: the relative energy change of electrons in a beam with flat distribution in aluminum chamber (left panel, solid line) and copper chamber (right panel, solid line). For comparison, we show by dashed lines (with the same correspondence between the color and the wall material) obtained for the energy change when one uses the EASE model of Ref. [3]. The dotted lines show the relative energy change for the case when the pipe is at room temperature. The vertical green lines indicate the rear edge of the bunch distribution: 30 μm for 100 pC and 90 μm for 300 pC.

are: for Cu $\eta_{\rm av} = -0.026\%$, $\sigma_\eta = 0.064\%$; for Al $\eta_{\rm av} = -0.023\%$, $\sigma_\eta = 0.049\%$.

The average energy loss $\eta_{\rm av}$ can be easily converted to the heating of the vacuum chamber walls. Denoting by P the power deposition per unit length of the chamber, we have $P = f_{\rm rep}|\eta_{\rm av}|EQ/eL$, where $f_{\rm rep}$ is the bunch repetition rate in the FEL. As an example, using $|\eta_{\rm av}| = 0.023\%$ for Al and the 300 pC beam and assuming $f_{\rm rep} = 1$ MHz, we obtain $P = 2.8$ W/m. This extra heating of the cold bore of the vacuum chamber should be taken into account in the design of the cryogenic system of the superconducting undulator.

In conclusion of this Section, we would like to point out that our results are rather insensitive to the exact choice of the value of RRR. To illustrate this insensitivity, we repeated calculations of the relative energy loss $\Delta E/E$ for two more values, RRR = 10 and RRR = 3 for Al. The last low value of RRR may be representative of Al alloys (see, e.g., [2], p. 466) that typically do not exhibit a strong ASE effect.

The comparison of the three different values of RRR is shown in Fig. 6. One can

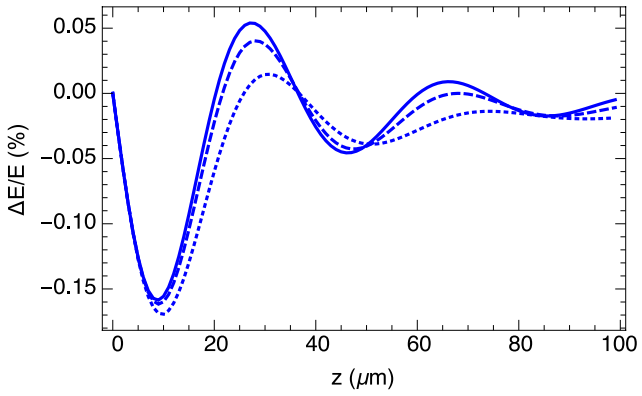

FIG. 6. Relative energy change for three values of RRR, for Al: the solid line is for RRR = 100, the dashed line is for RRR = 10, and the dotted line is for RRR = 3.

see that the large variations of the value of RRR result in a relatively small effect on the wakefield.

V. SUMMARY

In this paper we presented calculations of the longitudinal wakefields at cryogenic temperatures for extremely short bunches, characteristic for modern x-ray free electron lasers. The calculations are based on the equations for the surface impedance in the regime of the anomalous skin effect in metals. We find that, even though the metal conductivity at cryogenic temperatures may be two orders of magnitude higher than at the room temperature, the wakefield do not drastically differ in the two cases.

This work extends and complements an earlier analysis of Ref. [3] into the region of very high frequencies associated with bunch lengths in the micron range. We have studied in detail the case of a rectangular bunch distribution that often approximates well the realistic bunch profiles in FELs. This special kind of distri-

bution emphasizes the high-frequency content of the bunch spectrum, and require treatment that goes beyond simplifications accepted in [3].

VI. ACKNOWLEDGEMENTS

This work was supported by the Department of Energy, contracts DE-AC03-76SF00515 and DE-AC02-98CH1-886.

---

[1] A. W. Chao, *Physics of Collective Beam Instabilities in High Energy Accelerators* (Wiley, New York, 1993).

[2] A. W. Chao, K. H. Mess, M. Tigner, and F. Zimmermann, eds., *Handbook of accelerator physics and engineering*, 2nd ed. (Singapore, 2013).

[3] B. Podobedov, Phys. Rev. ST Accel. Beams **12**, 044401 (2009).

[4] P. Emma, N. Holtkamp, H.-D. Nuhn, D. Arbelaez, J. Corlett, S. Myers, S. Prestemon, R. Schlueter, C. Doose, J. Fuerst, Q. Hasse, Y. Ivanyushenkov, M. Kasa, G. Pile, E. Trakhtenberg, and E. Gluskin, in *Proceedings of the 2014 FEL Conference* (Basel, Switzerland, 2014).

[5] T. Raubenheimer, in *Proceedings of the 2014 FEL Conference* (Basel, Switzerland, 2014).

[6] G. E. H. Reuter and E. H. Sondheimer, Proceedings of the Royal Society of London A: Mathematical, Physical and Engineering Sciences **195**, 336 (1948).

[7] R. Dingle, Physica **19**, 311 (1953).

[8] A. P. Lenham and D. M. Treherne, J. Opt. Soc. Am. **56**, 752 (1966).

[9] C. Kittel, *Introduction to Solid State Physics*, 8th ed. (John Wiley & Sons, Inc., New York, 2005).

[10] L. D. Landau and E. M. Lifshitz, *Electrodynamics of Continuous Media*, 2nd ed., Course of Theoretical Physics, Vol. 8 (Pergamon, London, 1960) (Translated from the Russian).

[11] K. L. F. Bane and M. Sands, in *Micro Bunches Workshop*, AIP Conference Proceedings No. 367, edited by E. B. Blum, M. Dienes, and J. B. Murphy (AIP, New York, 1996) p. 131.

[12] K. Bane, G. Stupakov, and J. Tu, in *Proceedings of the 28th International Free Electron Laser Conference (FEL 2006)* (Edinburgh, UK, 2006) p. 2955.

[13] K. L. F. Bane and G. V. Stupakov, Phys. Rev. ST Accel. Beams **6**, 024401 (2003).

[14] K. Bane and G. Stupakov, in *Proceedings of the 2005 Particle Accelerator Conference* (Knoxville, Tennessee USA, 2005) p. 3390.